GLL
Geomatics, Landmanagement and Landscape No. 1 • 2025, 19–41

ISSN 2300-1496 https://doi.org/10.15576/GLL/201222

Research paper

Received: 22.11.2024
Accepted: 14.01.2025
Published: 31.03.2025

Assessment and mapping of areas at risk of flooding using a combined AHP and GIS multi-criteria analysis model – case study of Sidi Aissa city (Algeria)

Mohammed Ben Halima[1, ✉] 0009-0007-2476-3060
Ali Redjem[1] 0000-0001-8527-397X
Salim Dehimi[1] 0000-0002-2888-2397
Abdelkrim Bensaid[2] 0000-0002-7616-6184

[1] City, Environment, Hydraulics and Sustainable Development Laboratory, Urban Technology Management Institute, University of Mohamed Boudiaf, M'sila, Algeria
[2] Cedete Laboratory, UFR LLSH, Department of Geography, University of Orléans, France
✉ Corresponding author: mohammed.benhalima@univ-msila.dz

Summary

Floods are among the most hazardous natural disasters, which pose significant threats to human lifeat both global and national scales due to severe human, material, and environmental losses. The increasing frequency of floods, compared to other natural hazards, highlights the urgent need of their evaluation and the mitigation of their impacts. This study aimed to assess and map flood-prone areas in the city of Sidi Aissa, Algeria, using the analytical hierarchy process (AHP) and geographic information systems (GIS). The city was chosen because of the three rivers running through it. A model combining a multi-criteria statistical approach and GIS was employed. The study focused on analyzing the factors influencing flood occurrence, including land use, elevation, slope, drainage density, distance from river and roads, topographic wetness index (T.W.I), and normalized difference vegetation index (N.D.V.I), To calculate the weights of these factors in the GIS environment, the AHP method was applied, resulting in maps specific to each criterion. The results revealed that land use (21.7%) and distance from river (18.2%) are the most critical factors influencing flood susceptibility and damage to nearby buildings. The study shaped a flood susceptibility map divided into three categories: areas with very low flood susceptibility, accounting for 29% of the total area; areas with moderate flood susceptibility, accounting for 40% and areas highly susceptible to flooding, making up 31%. Furthermore, the study demonstrated the effectiveness of using AHP and GIS in simulating potential floods and identifying flood-prone areas, thereby highlighting their importance in planning and mitigating flood risks in the future.

Keywords

Analytical Hierarchy Process (AHP) • Geographic Information Systems (GIS) • floods • vulnerability • Sidi Aissa • criteria

1. Introduction

Floods in urban areas present significant risks to populations, particularly with the rapid urban expansion observed in recent years. Development along riverbanks often disregards recommended building setbacks and urban planning regulations, exacerbating the problem. According to Cabrera and Lee [2020], financial losses from floods account for approximately 40% of all annual economic damage related to natural hazards.

The recent decades have witnessed a notable increase in flood events worldwide, leading to a significant rise in associated fatalities. The World Health Organization (WHO) reports that approximately 75% of all natural disaster-related deaths are attributed to flooding, underscoring its growing impact on public health and the environment. Factors such as urban sprawl and climate change contribute to the increasing frequency and severity of floods, affecting regions such as Central Asia, Africa, Southeast Asia, and Central Europe [WHO Report 2023].

To mitigate these challenges, decision-makers have developed innovative techniques for flood forecasting, preparedness, and risk reduction strategies [Haltas et al. 2021]. Flood risk maps serve as critical tools for identifying vulnerable areas and guiding future urban development strategies [Buchele et al. 2006]. Such mapping efforts require multi-criteria analysis and collaboration among stakeholders with geographic relevance [Poussin et al. 2014].

Geographic Information Systems (GIS) and remote sensing technologies have significantly advanced natural hazard analysis [Patel and Srivastava 2013]. These tools have facilitated studies on flood hazard sensitivity and flood event simulation [White et al. 2010].

Multi-criteria analysis (MCA) is a robust tool for evaluating complex decisions involving non-quantifiable criteria [Malczewski 2006]. It integrates technical, environmental, and socio-economic objectives to support optimal decision-making [Ghanbarpour et al. 2013]. The AHP method, which relies on expert judgment for assigning weights, is particularly effective in addressing complex multi-criteria decisions in disaster management [Rozos et al. 2011].

Flooding is one of the most common natural disasters in Algeria, recurring in many regions due to climate variability and inadequate infrastructure. This study aims to develop a flood vulnerability map for the city of Sidi Aissa using AHP and GIS methods. Selecting evaluation criteria is critical for disaster planning and management, significantly enhancing the accuracy of flood risk assessments.

This study relies on elements found in previous research for their applicability to flood mapping, given the lack of agreement among academics over the criteria for evaluating flood danger. In order to determine the most important variables influencing the occurrence of floods and to create efficient flood risk reduction plans, eight criteria were chosen.

2. Study area

The city of Sidi Aissa is situated at the westernmost edge of the Hodna Mountain range in the northwestern part of the M'sila Province, Algeria. It lies at the intersection of the National Road 60 and National Road 8, located at latitude 35°53'11"N and longitude 3°46'32"E. The municipality is part of the northwestern region of the Hodna Basin and covers an area of 49.46 km². It is bordered by the following:

- north: the Bouira Province (municipalities of Taguedit, Dirah, and Maamoura),
- east: the Bouira Province (municipality of Hajara Zerga),
- west: Sidi Aissa municipality,

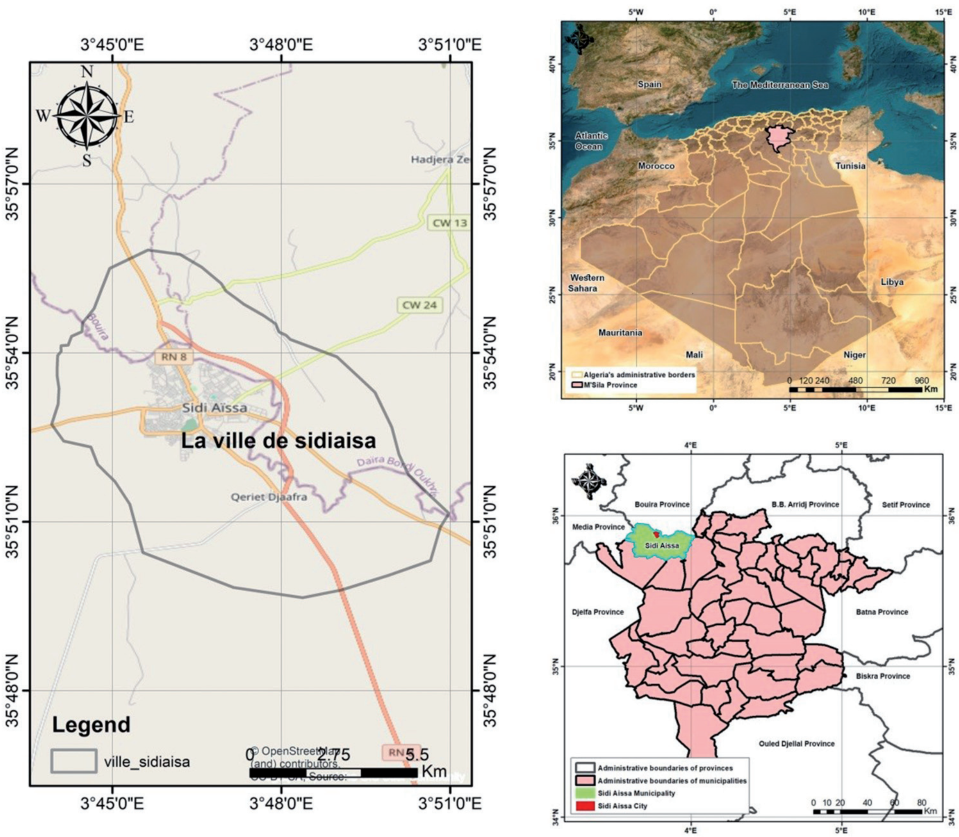

Source: Authors' own study, using ArcGIS (version 10.4) and OpenStreetMap

Fig. 1. Location of Sidi Aissa City, M'Sila, Algeria

- south: The village of Djafra (Master Plan for Development and Construction Sidi Aissa, 2008).

Sidi Aissa is located in a semi-flat area interspersed with several hills, particularly in zones designated for future urbanization. These hills have varying slopes according to the catchment areas feeding the three rivers (Ouads) traversing the city: Ouad Qatrini, Ouad Djennan, and Ouad Lahm.

The rivers significantly affect the functional relationships between different parts of the city, and act as barriers to these interactions. Bridges have been proposed as connections across the river, but they pose significant economic challenges.

3. Previous studies

A bibliometric analysis approach was adopted for this study, focusing on keywords frequently used in highly cited academic articles and journals. Tools like RStudio, known for bibliometric network visualization, were employed to map the relationships between key topics.

This review explored the connection between flooding, AHP analysis, and GIS. A systematic review of documented literature was conducted, highlighting approximately 149 studies from 2013 to 2023, which reflects the growing interest in this field.

This type of analysis provides valuable insights into the studied topic and enhances understanding of the relationship between floods and risk management by utilizing techniques such as the analytic hierarchy process (AHP) and geographic information systems (GIS) (Fig. 2).

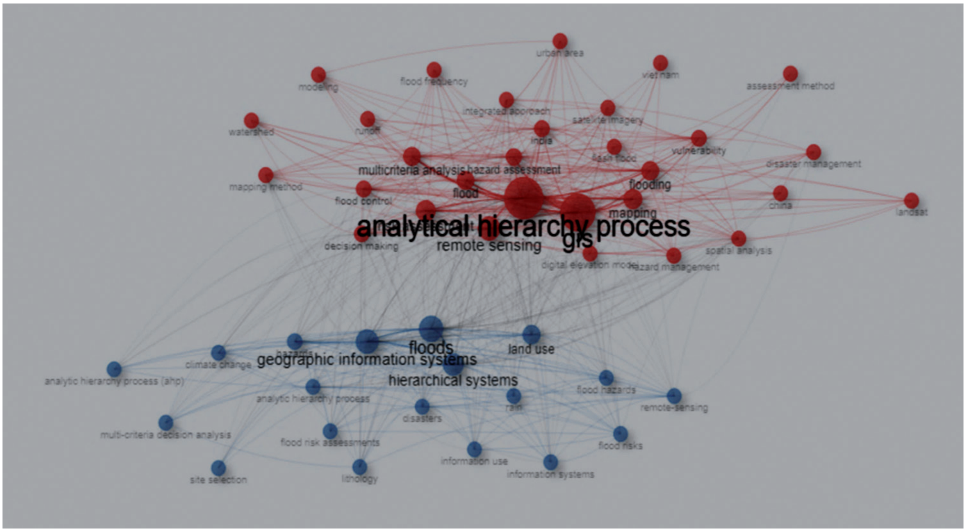

Source: RStudio (version R 3.6.0)

Fig. 2. A network visualization of the research topic

Figure 2 illustrates a network visualization of concepts and key terms related to research on floods, such as the analytic hierarchy process (AHP) and geographic information systems (GIS). This type of visualization is commonly used in bibliometric analysis to highlight the relationships between different research topics based on citation patterns or keyword co-occurrences.

3.1. Key observations from the visualization

Core topics

- Terms such as 'hierarchical analysis' and 'geographic information systems' are dominant, indicating their importance in flood studies.
- Other keywords are concepts such as 'flooding,' 'remote sensing,' and 'multi-criteria analysis' that frequently co-occur with AHP and GIS.

Connections

- The links between keywords highlight their interrelation in literature, showing a high level of interaction.

Research areas

- Keywords related to 'disaster management', 'land use', and, 'vulnerability' indicate a multidisciplinary approach that encompasses environmental science, urban planning, and emergency management.

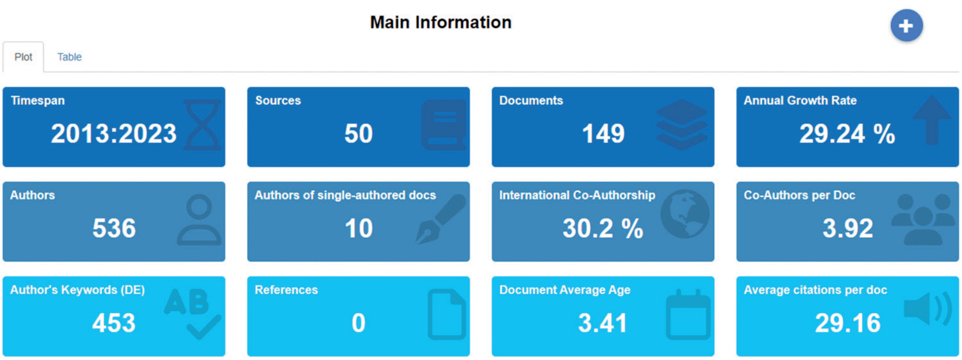

Source: RStudio (version R 3.6.0)

Fig. 3. Statistical data of studies on the research topic

These analyses help researchers identify trends within specific fields, understand the existing research landscape, and uncover gaps that may warrant further investigation. Additionally, they enhance decision-making processes by providing a clearer understanding of the interactions among various variables.

The results presented in the table indicate that the analytical hierarchy process (AHP) and geographic information systems (GIS) in relation to flood phenomena have been extensively studied by numerous researchers across various regions worldwide. These studies have utilized diverse techniques and methodologies in order to simulate floods, map flood-prone areas, and minimize associated losses.

For example, Bitlis Province in Turkey's flood-prone areas were mapped using the AHP method in a GIS environment by Aydın and Sevgi Birincioğlu [2022]. Similarly, the Gagara river basin in Uttar Pradesh, India, and the Shangla region in Pakistan were mapped using a multi-criteria analysis in a GIS context.

Additionally, researchers such as Desalegn and Mulu [2021], Hagos et al. [2022], Negese et al. [2022], and Ogato et al. [2020] have integrated AHP and GIS-based multi-criteria analysis to assess flood risks and develop flood susceptibility maps in various parts of the world.

The studies demonstrate that the main criteria used for flood mapping include elevation, slope, land cover type, rainfall, drainage density, soil types, and distance from to rivers. Some studies also consider additional factors, such as the normalized difference vegetation index (NDVI) and the topographic wetness index (TWI).

However, the lack of hydrometeorological data in developing countries poses a significant challenge to flood susceptibility mapping, adversely affecting the ability to make informed decisions and engage in effective emergency planning [Allafta and Opp 2021, Cabrera and Lee 2018].

Table 1. Factors influencing floods used in previous studies for mapping hazard-prone areas

Literature	**Distance from sewer drainage**	**Topographic wetness index**	**Elevation**	**Slope**	**Rainfall**	**Land cover**	**Normalized difference vegetation index**	**Distance from river**	**Distance from road**	**Drainage density**	**Soil types**
Richard et al. [2023]		✓	✓	✓	✓	✓		✓		✓	
Bikila Merga Letaan et al. [2023]	✓	✓	✓	✓	✓	✓	✓	✓	✓	✓	✓
Aydin and Sevgi Birincioğlu [2022]			✓	✓	✓	✓		✓			
Edamo et al. [2022]		✓	✓		✓	✓		✓		✓	✓
Hagos et al. [2022]			✓	✓	✓	✓		✓		✓	✓
Negese et al. [2022]		✓	✓	✓	✓	✓	✓	✓		✓	✓
Ramesh and Iqbal [2022]	✓	✓	✓	✓		✓					✓
Nsangou et al. [2022]		✓	✓	✓	✓	✓		✓		✓	

Desalegn and Mulu [2021]			✓	✓	✓	✓				✓	✓
Arya and Singh [2021]				✓	✓	✓				✓	✓
Das and Gupta [2021]		✓	✓	✓	✓	✓		✓		✓	✓
Hussain et al. [2021]			✓	✓	✓	✓					
Roy et al. [2021]		✓	✓	✓	✓			✓		✓	✓
Ajibade et al. [2021]		✓	✓	✓							
Allafta and Opp [2021]			✓	✓	✓	✓		✓		✓	
Abdelkarim et al. [2020]				✓	✓	✓				✓	
Arshad et al. [2020]			✓		✓	✓				✓	✓
Dash and Sar [2020]			✓	✓	✓	✓				✓	
Ullah and Zhang [2020]		✓	✓	✓	✓	✓		✓		✓	
Ogato et al. [2020]			✓	✓	✓	✓	✓				✓
Subbarayan and Sivaranjani [2020]			✓	✓	✓			✓		✓	
Chakraborty and Mukhopadhyay [2019]			✓	✓	✓	✓				✓	
Gambini and Laymito [2019]			✓	✓	✓	✓		✓		✓	
Hoque et al. [2019]			✓	✓	✓	✓		✓			✓
Rahman et al. [2019]			✓	✓	✓	✓			✓		
Cabrera and Lee [2018]			✓	✓	✓			✓		✓	✓
Ghosh and Kar [2018]			✓	✓	✓			✓			✓
Rincón et al. [2018]			✓	✓	✓			✓			
Bulti et al. [2017]			✓	✓		✓				✓	

D.S.D distance from sewer drainage, **T.W.I** topographic wetness index, **El** elevation, **Sl** slope, **Rf** rainfall, **L.C** land cover, **N.D.V.I** normalized difference vegetation index, **D.River** distance from river, **D.road** distance from road, **D.D** drainage density, **S.T** soil types

Source: Collection of previous studies

4. Materials and methods

This study utilised multi-criteria analysis (MCA) and the analytical hierarchy process (AHP) in conjunction with geographic information systems (GIS) to assess and accurately delineate flood-prone regions. The AHP-GIS methodology was selected for this study because of its suitability for data-deficient contexts and its ability to effectively combine quantitative and qualitative data.

In contrast to machine learning methods that necessitate large training datasets, the AHP-GIS approach offers a transparent decision-making framework that integrates expert judgement, rendering it especially suited for scientific research.

Although machine learning approaches can provide superior forecast accuracy, their implementation is sometimes limited by data availability and processing resources, a constraint particularly pertinent in our location. We recognise the potential significance of these methods and advocate for their investigation in subsequent research to corroborate and improve our results.

The analysis carefully examined the context of the study site, incorporating field observations, expert opinions, local inhabitants' viewpoints, and a comprehensive review of relative literature. This process revealed eight critical elements that substantially influence flood susceptibility, which are:

- topographic wetness ondex (TWI),
- elevation (E),
- slope (S),
- land use and land cover (LULC),
- normalized difference vegetation index (NDVI),
- distance from rivers (D.River),
- distance from roads (D.Roads),
- drainage density (D.D).

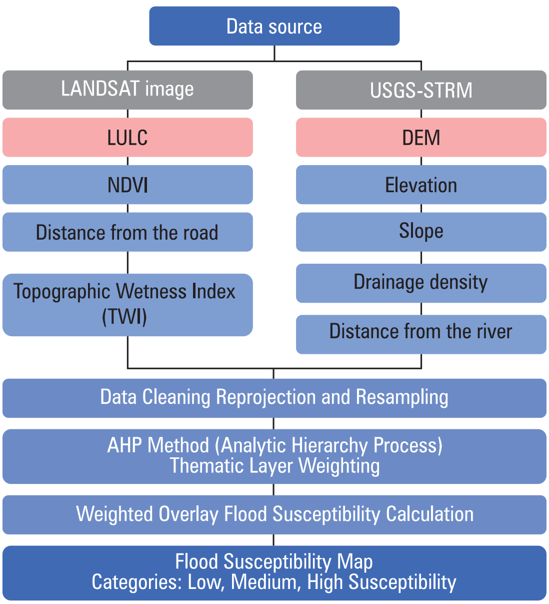

Source: Authors' own study

Fig. 4. Flow chart of flood susceptibility map by GIS method

These factors were classified on a susceptibility scale from very low (1) to very high (5). Reclassification was performed in the GIS environment using the Reclassify tool and analyzed through a 10×10 m for Sentinel-2 data resolution raster grid in the WGS_1984_UTM_Zone_31N coordinate system. AHP was applied to assign relative weights to each criterion, with data layers combined using a weighted overlay analysis in ArcGIS (version 10.4) to produce a flood susceptibility map. Microsoft Excel was extensively used for the AHP computations.

4.1. Method of analytical hierarchy processing (AHP)

Multi-criteria decision-making problems in flood analysis were prioritized using AHP approaches created by [Saaty 1987]. AHP was used for multi-criteria decision-making in the analysis of urban flood-prone areas by a number of researchers, including Balica et al. [2012], Lin et al. [2019], Negese et al. [2022] and Ramesh and Iqbal [2022]. In order to ascertain the relative significance of flood-related parameters, the AHP analysis was conducted. This procedure entailed consistency verification once the pairwise comparison matrix (Table 4) was constructed. Each element was reclassified, and then further analysis was done. The following methods were used to ascertain the relative weights of each factor, per Saaty [1987] advice:

- Pairwise comparison matrix: developed based on Saaty's scale (1–9) for comparing the relative importance of each criterion (Table 2).
- Each entry in the specified pairwise comparison matrix was then divided by the sum of its corresponding column (Table 4).
- After calculating the weights of each factor related to flood exposure, the consistency index (CI) was computed using the following equation developed by Saaty [1987]:

$$\mathrm{CI} = \frac{\lambda_{\max} - n}{n - 1}$$

where:
CI – consistency index,
N – number of factors to be examined,
λ_{max} – maximum eigenvalue of a pairwise comparison matrix.

Table 2. Saaty's scale of pairwise comparisons

Intensity of importance	Degree of preference	Explanation
1	Equal importance	Two components equally contribute to the goal.
3	Moderate importance	One parameter is marginally preferred over another by experience and judgment.
5	The strong or essential importance	Experience and judgment strongly favor one activity over another.

Table 2. cont.

Intensity of importance	Degree of preference	Explanation
7	Very strong importance	One parameter is significantly favored and regarded as superior to another; its domination is evidenced in practice.
9	Extreme importance	The strongest possible order of affirmation is found in the evidence supporting one parameter over another.
2,4,6,8	Intermediate values	When factors that are of similar importance.

Source: Saaty [1977]

- Subsequently, each entry in the specified pairwise comparison matrix was divided by the corresponding column sum (Table 6).

To calculate the maximum eigenvalue (λ_{max}) of the pairwise comparison matrix, the following steps were followed [Saaty 1987]:

- Each column value in the matrix was multiplied by the corresponding weight criteria.
- The row values are summed to calculate the weighted total.
- Each criterion value is weighted based on its weighted total.
- The weighted sum of the mean is calculated with respect to the criterion weights.

The consistency ratio (CR) was then calculated to assess the validity of the comparison, as proposed by Saaty [1987], using the following equation:

$$CR = \frac{CI}{RI}$$

Saaty [1987] states that the pairwise comparison matrix is deemed consistent if the consistency ratio (CR) is less than 0.10. The procedure must be repeated until the CR value drops below this cutoff, since if it is larger than or equal to 0.10, there is inadequate consistency. Based on the matrix size, the consistency index (CI) equation yielded a random consistency index (RI) (Table 3).

Table 3. Random consistency index for values of N

Size of matrix	1	2	3	4	5	6	7	8	9	10
Random consistency index	0	0	0.58	0.9	1.12	1.24	1.32	1.41	1.45	1.49

Source: Saaty [1987]

5. Results and discussion

5.1. Flood conditioning factors

Table 6 includes data on the factors contributing to floods (their units, categories, susceptibility, classification values, and weight for the study area), which were analyzed using ArcGIS (version 10.4) for multi-criteria decision-making and analytical hierarchy process.

Table 4. Pairwise comparison matrix for selected flood conditioning factor

Thematic layer	Topographic Wetness Index (TWI)	Elevation	Slope	LULC	NDVI	Distance from river	Distance from road	Drainage density
Topographic Wetness Index (TWI)	1	1	1	0.33	19	0.25	1	1
Elevation	1	1	1	0.33	1	0.5	3	2
Slope	1	1	1	0.5	2	0.5	1	2
LULC	3	3	2	1	1	2	3	2
NDVI	1	1	0.5	1	1	2	3	2
Distance from river	4	2	2	0.5	0.5	1	3	3
Distance from road	1	0.33	1	0.33	0.33	0.33	1	1
Drainage density	1	0.5	0.5	0.5	0.5	0.33	1	1
	14	10	9	4.49	7	6.91	16	14

Source: Authors' own study based on the Saaty matrix

Table 5. Consistency check results

λ_{max}	N	CI	RI	CR
8.60	8	0.086	1.41	0.061

Source: Authors' own study

Table 6. Flood conditioning factors: weight, rating values, flood susceptibility, and their classes

Flood conditioning factors	Class	Flood susceptibility	Susceptibility rating	Weight [%]
Topographic Wetness Index (TWI)	1.36–3.16	Very low	1	8.4
	3.17–5.05	Low	2	
	5.06–7.35	Moderate	3	
	7.36–10.6	High	4	
	10.7–19.8	Very high	5	

Table 6. cont.

Flood conditioning factors	Class	Flood susceptibility	Susceptibility rating	Weight [%]
Elevation [m]	646–690	Very high	5	11.3
	690–730	High	4	
	730–770	Moderate	3	
	770–810	Low	2	
	810–849	Very low	1	
Slope [%]	0–4	Very high	5	11.9
	5–8	High	4	
	9–10	Moderate	3	
	11–20	Low	2	
	30–80	Very low	1	
LULC (class)	Green Area	Very high	3	21.7
	Urban Area	Moderate	5	
	Barren Area	Very low	1	
NDVI	108–112	Very high	5	15.2
	112–119	High	4	
	119–129	Moderate	3	
	129–140	Low	2	
	140–154	Very low	1	
Distance from river [m]	0–500	Very high	5	18.2
	500–1000	High	4	
	1000–1500	Moderate	3	
	1500–2000	Low	2	
	2000–3100	Very low	1	
Distance from road [m]	0–25	Very high	5	6.5
	25–50	High	4	
	50–100	Moderate	3	
	100–300	Low	2	
	300–420	Very low	1	

Drainage density [km/km^2]	0–1.6	Very low	1	6.8
	1.7–3.2	Low	2	
	3.3–4.8	Moderate	3	
	4.9–6.4	High	4	
	6.5–8	Very high	5	

Source: Authors' own study

5.2. Topographic Wetness Index (TWI)

This index represents the spatial distribution of soil moisture and surface saturation, and is crucial for describing the hydrological similarity of flood-prone areas by controlling the area's topography during hydrological processes [Waga et al. 2020]. Areas with a high TWI are more prone to flooding, while areas with a low TWI are less likely to flood [Paul et al. 2019]. The TWI was calculated by the ASTER DEM using the following equation:

$$\mathrm{TWI} = \mathit{In}\left(\frac{\mathrm{AS}}{\tan\beta}\right)$$

where the contributing area upstream is denoted by AS, and the slope gradient is denoted by β. The final TWI map was divided into five categories, ranging from 1.36 to 19.6 (Fig. 5).

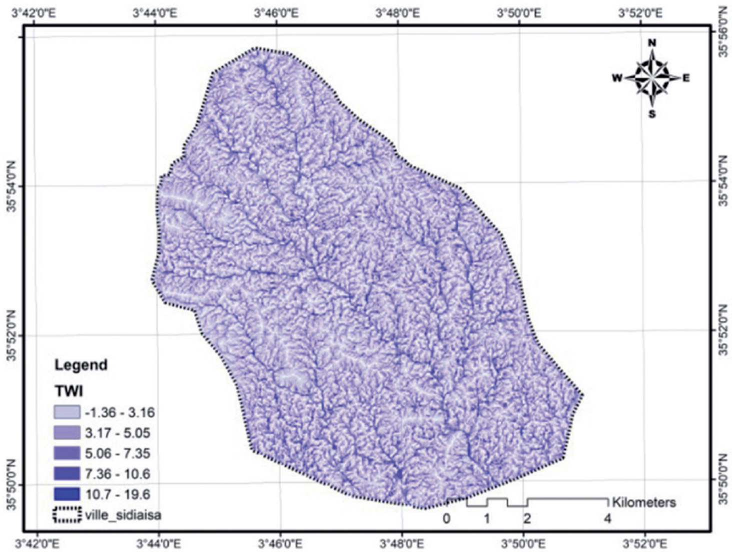

Source: Authors' own study, using ArcGIS (version 10.4)

Fig. 5. Topographic Wetness Index

5.3. Elevation

Elevation is a key factor in assessing flood exposure [Rahmati et al. 2016, Das 2019, Shen et al. 2021]. Water typically flows from higher to lower areas due to elevation, which can result in rapid flooding of low-lying regions. The likelihood of flooding is higher in low-elevation areas compared to higher elevations [Das 2018, Liuzzo et al. 2019, Elkhrachy 2022]. The elevation map for the study area was created using the ASTER DEM and spatial analysis tools in the ArcGIS environment. As shown in Figure 6, the elevation of the study area ranges from 646 to 849 meters above sea level.

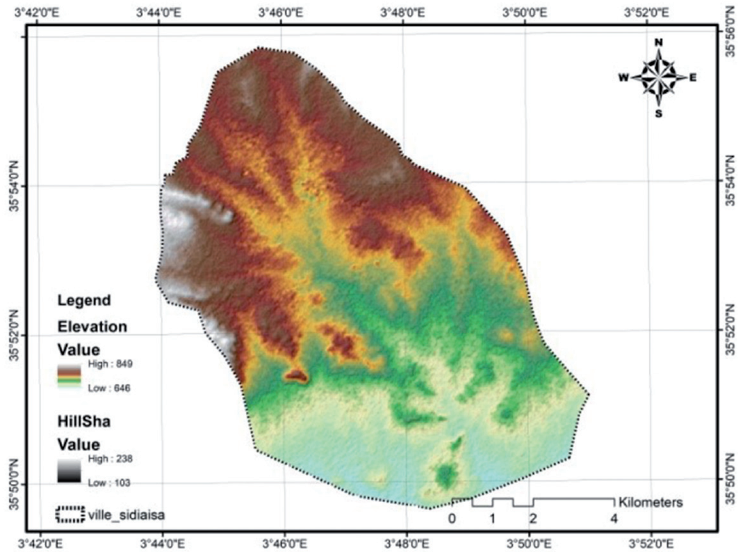

Source: Authors' own study, using ArcGIS (version 10.4)

Fig. 6. Elevation

5.4. Slope

Slope is one of the most important factors in hydrological studies, as it controls surface runoff and the density of water flow, which in turn promotes soil erosion and vertical seepage processes [Tehrany et al. 2015, Khosravi et al. 2016b]. Areas with steeper slopes have lower flood exposure, while areas with gentler slopes are more susceptible to flooding [Liuzzo et al. 2019]. The slope map was derived from the ASTER DEM with a 30-meter resolution using the Slope tool in ArcGIS, and it was classified into five subcategories, ranging from 0° to 80° (Fig. 7).

5.5. Land use

Land use/land cover (LULC) plays a vital role in the water runoff process and the occurrence of floods in a watershed area [Riazi et al. 2023]. The strong relationship between land use, climate change, and floods is undeniable, as land use and land cover significantly influence the increase or reduction of water flow [Samanta et al. 2018]. LULC data were collected from the ESRI 2023 global land use and land cover database and classified into three categories: grassland, built-up areas, and barren land (Fig. 8).

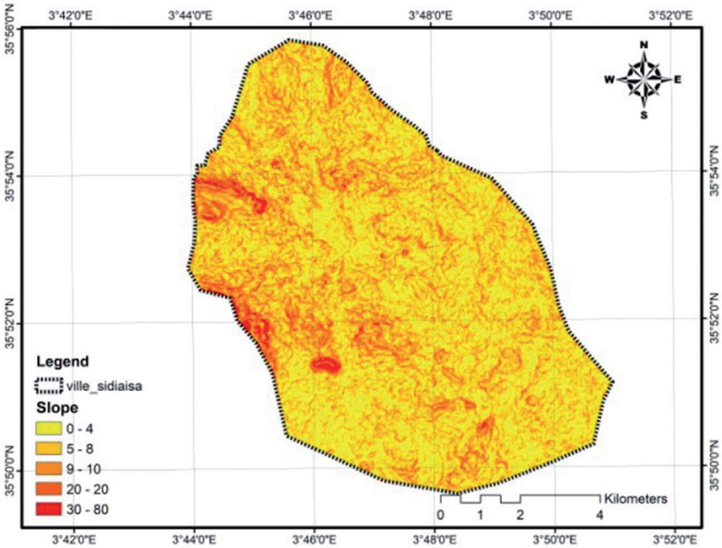

Source: Authors' own study, using ArcGIS (version 10.4)

Fig. 7. Slope

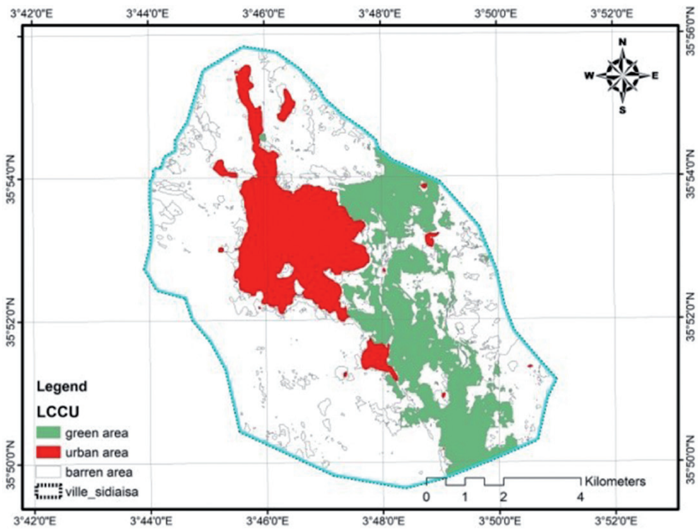

Source: Authors' own study, using ArcGIS (version 10.4)

Fig. 8. Land use

5.6. Normalized difference vegetation index (NDVI)

The normalized difference vegetation index (NDVI) is another key environmental factor that contributes to flooding. The natural range of NDVI values is from 0.1 to +1 [Khosravi et al. 2016b, Riazi et al. 2023]. Positive NDVI values indicate active vegetation cover, such as dense forests, while values close to zero represent arid regions, and negative values indicate water bodies [Wang et al. 2020, Ziwei et al. 2023]. To generate the NDVI map, satellite data from the Landsat 8.1 collection, provided by the USGS, were used, and the NDVI value was calculated using the following equation:

$$\mathrm{NDVI} = \frac{\mathrm{NIR} - \mathrm{Red}}{\mathrm{NIR} + \mathrm{Red}}$$

where NIR represents near-infrared light and RED is visible light. The NDVI map for the SRB was classified into five subcategories ranging from 0.11 to 0.15 using the natural breaks tool (Fig. 9).

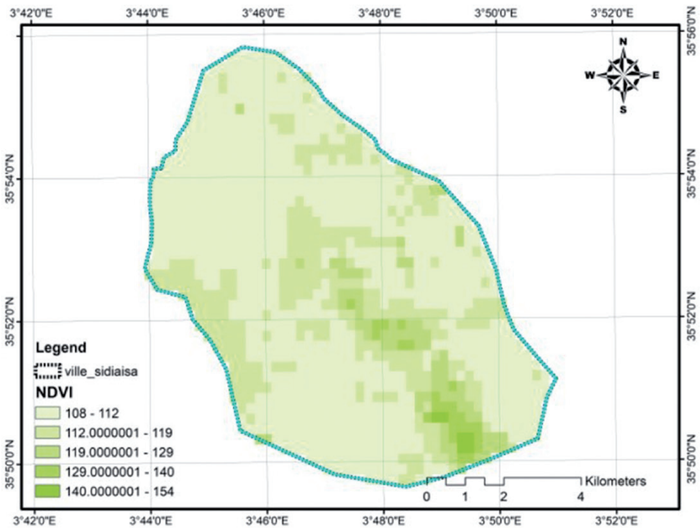

Source: Authors' own study, using ArcGIS (version 10.4)

Fig. 9. Normalized difference vegetation index

5.7. Distance from the river

As shown in Figure 10 and Table 6, the distance from the river in the study area was classified into five categories: very high, high, moderate, low, and very low flood susceptibility at distances of 500 m, 1000 m, 1500 m, 2000 m, and > 2000 m, respectively. Based on the map, it is evident that a significant portion of the study area is prone to moderate to very high flood susceptibility due to its distance from river.

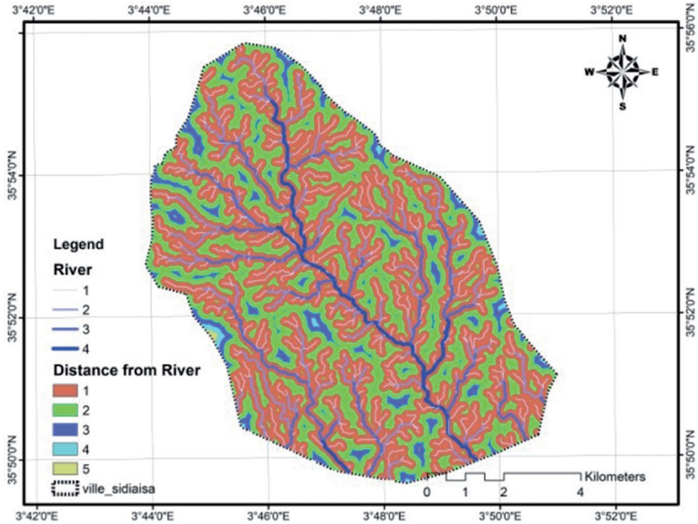

Source: Authors' own study, using ArcGIS (version 10.4)

Fig. 10. Distance from the river

5.8. Distance from the road

The distance from the road in the study area was classified into five categories: very high, high, moderate, low, and very low flood susceptibility at distances of 25 meters, 50 meters, 100 meters, 300 meters, and > 300 meters, respectively (Fig. 11).

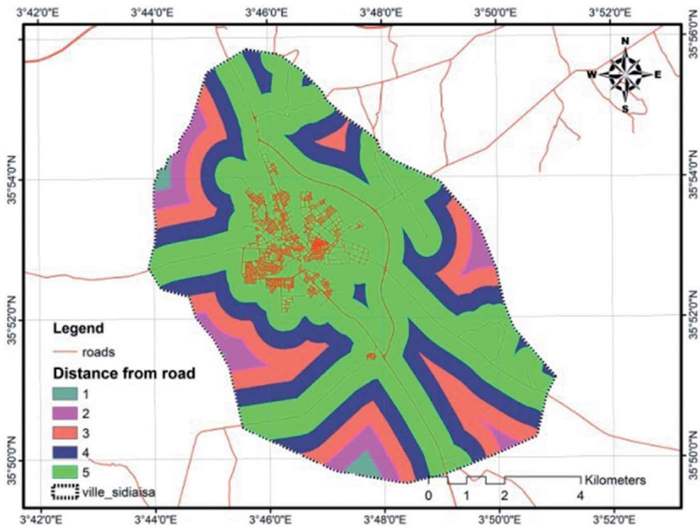

Source: Authors' own study, using ArcGIS (version 10.4)

Fig. 11. Distance from the road

The results of the study revealed that a large area near roads is at risk of flooding due to its low environmental capacity for water infiltration through the surface layers of the soil. Impervious surfaces, such as roads, reduce infiltration capacity and increase surface runoff by limiting the ability of rainwater to seep into the soil, thus having a significant impact on flooding in urban areas.

5.9. Drainage density

Drainage density is defined as the total length of rivers and streams in a watershed divided by the total area of the watershed [Rahmati et al. 2016]. Areas with high drainage density have a higher likelihood of flooding, while areas with low drainage density have a lower likelihood of flooding [Paul et al. 2019]. Drainage density measures the efficiency of water drainage within the watershed through streams.

To calculate drainage density in the study area, the flow order was extracted from the ASTER DEM using the Line Density tool in the ArcGIS environment, and classified into five categories using the Natural Breaks (Jenks) tool (Fig. 12). The following equation was used to calculate drainage in the study area:

$$\mathrm{Dd} = \frac{\sum_{1}^{N} \mathrm{L}}{\mathrm{A}}$$

where drainage density is denoted by the symbol Dd, the length of watercourses is denoted by L, and the total area of the watershed is denoted by A.

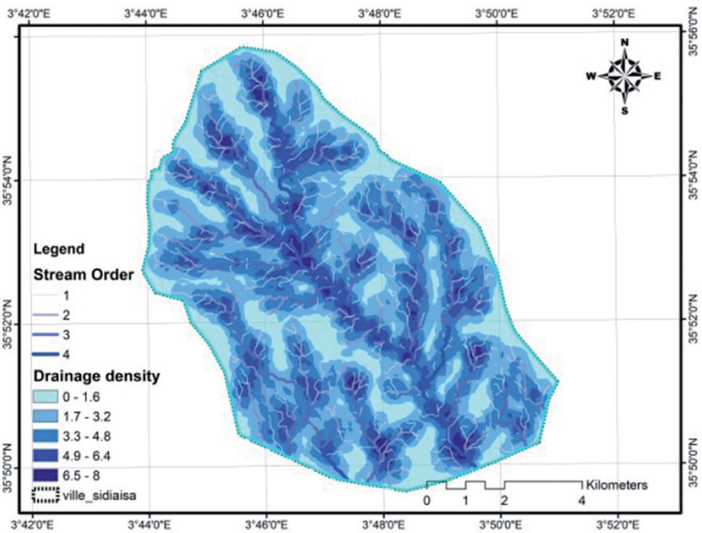

Source: Authors' own study, using ArcGIS (version 10.4)

Fig. 12. Drainage density

The drainage density for the study area ranged from 1.6 to 8, and was classified into five categories: 0 – 1.6 (very low), 1.7 – 3.2 (low), 3.3 – 4.8 (moderate), 4.9 – 6.4 (high), and 6.5 – 8 (very high), as shown in Figure 12. The results revealed that the study area is highly susceptible to flooding, with 57% of the study area at risk of flooding due to high drainage density and low infiltration that may accelerate water flows causing flooding events.

6. Flood susceptibility map

The analytical hierarchy process (AHP) was used to create the eight maps, which were then integrated and overlaid in a GIS environment. Flood-prone areas were identified and supported by the flood susceptibility map, with historical flood data validating the methodology. A final flood-sensitive map was developed and divided into five main flood potential levels, ranging from very low to very high, as shown in Table 7.

According to the weights derived from the AHP approach, the study parameters are linearly integrated. In the GIS environment, based on the equation (provided below), thematic layers are overlaid with different weights. The flood susceptibility index (FSI) for each pixel within the study area was then calculated. R represents the rank, and W represents the weight of the thematic layers.

$$FSI = R_{TWI} \cdot W_{TWI} + R_{EL} \cdot W_{EL} + R_{SL} \cdot W_{SL} + R_{LULC} \cdot W_{LULC} + R_{NDVI} \cdot W_{NDVI} + \\ + R_{DF} \cdot W_{DF} + R_{DR} \cdot W_{DR} + R_{DD} \cdot W_{DD}$$

The results of the study were categorized into three classes: very low, covering 29% of the area; moderate, covering 40% of the area; and very high, covering 31% of the area (Fig. 12). The flooding phenomenon was influenced by the parameters with higher weights, while it was less affected by parameters with smaller weights. As a result, these findings provide essential data that should be considered in flood management.

Table 7. Classification of flood susceptibility zone

Classification	Total area covered [km^2]	Area percentage [%]
Very low	14.19	29
Medium	19.83	40
Very high	15.44	31

Source: Authors' own study

The study primarily emphasises environmental and topographical factors in the flood risk analysis, indicating that infrastructure, including drainage channels, roads, and bridges, were evaluated based on proximity to roads and rivers, as the design of these structures influences drainage capacity and water flow management. Despite the significance of economic analysis in assessing the feasibility of interventions from a cost-benefit perspective, it was excluded from this study due to several constraints. This research necessitates the availability of precise and comprehensive economic data, which proved challenging to get within the constraints of this study. Moreover, an accurate economic evaluation requires a detailed economic model founded on several assumptions and intricate economic factors, which requires more time and money.

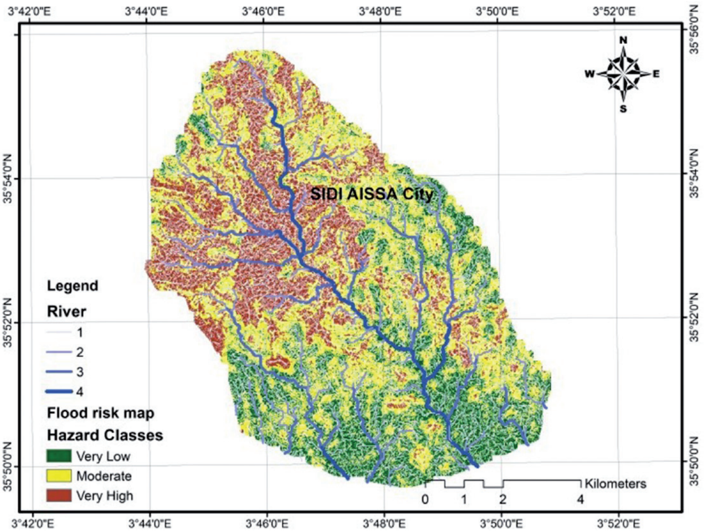

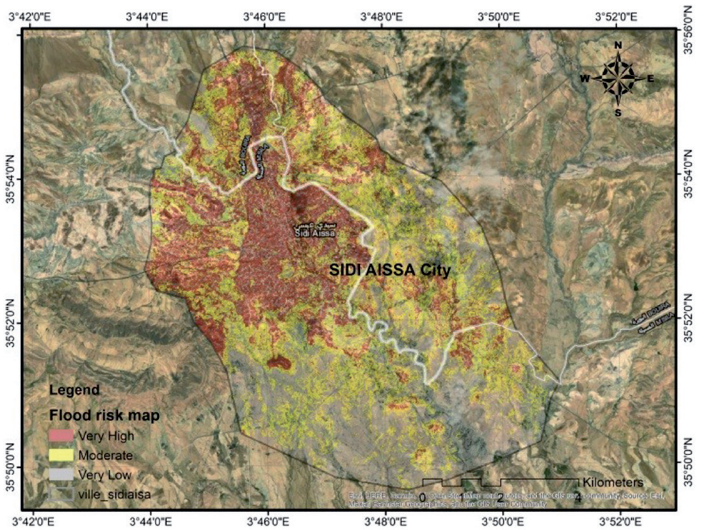

Source: Authors' own study, using ArcGIS (version 10.4)

Fig. 13. and **14.** Map of flood-prone areas in the study area

Owing to constraints in the accessible data, a comprehensive analysis of the current infrastructure status could not be incorporated into this study. Therefore, emphasis was made on the technical and scientific dimensions to ensure the delivery of appropriate engineering and environmental solutions.

7. Conclusion

In conclusion, this study on the assessment and mapping of flood-prone areas using multi-criteria hierarchical analysis and geographic information systems (GIS) in the city of Sidi Aissa, Algeria, highlights the importance of adopting these modern tools for analyzing and processing environmental and geographical data related to natural disasters. The study demonstrated that integrating hierarchical analysis with GIS is an effective approach for identifying and classifying areas at highest risk of flooding.

The results revealed that distance from river and land use are the most influential factors increasing the likelihood of flooding. In particular, 31% (14.19 km^2) of the classified area was highly susceptible to flooding, 40% (19.83 km^2) was classified as moderately exposed to flooding, indicating the need for preventive measures to reduce the risk in these areas, while areas with very low exposure accounted for 29% (15.44 km^2) of the city's total area.

The use of a range of influential criteria, including elevation, slope, drainage density, distance from river, and land use, significantly improved the accuracy of predictive models. This approach not only enhances disaster management strategies but also provides practical solutions for sustainable urban planning and land use in the city.

Thanks to the results of this study, local authorities can now direct their efforts toward protecting infrastructure and minimizing human and material losses. The study also underscores the importance of adopting such analyses as a tool for urban planning and disaster management on a broader scale, which strengthens communities' resilience to climate change and recurrent flooding.

In summary, this model provides a practical framework that can be applied to other regions similar to Sidi Aissa, thereby increasing the effectiveness of future planning and disaster response strategies.

References

Allafta H., Opp C. 2021. GIS-based multi-criteria analysis for flood prone areas mapping in the trans- boundary Shatt Al-Arab basin, Iraq-Iran. GeomaticsNatl Hazards Risk, 12(1), 2087–2116.

Aydin M.C., Sevgi Birincioğlu E. 2022. Flood risk analysis using GIS based analytical hierarchy process: a case study of Bitlis Province. Appl. Water Sci., 12(6), 122.

Balica S.F., Wright N.G., Van der Meulen F. 2012. A flood vulnerability index for coastal cities and its use in assessing climate change impacts. Nat Hazards, 64, 73–105.

Cabrera J.S., Lee H.S. 2018. Impacts of climate change on flood-prone areas in Davao Oriental, Philippines. Water, 10(7), 893.

Das S. 2018. Geographic information system and AHP-based flood hazard zonation of Vaitarna basin, Maharashtra, India. Arabian J. Geosciences, 11, 576. https://doi.org/10.1007/s12517-018-3933-4

Das S. 2019. Geospatial mapping of flood susceptibility and hydro-geomorphic response to the floods in Ulhas basin, India. Remote Sens. Appl., 14, 60–74. https://doi.org/10.1016/j.rsase.2019.02.006

Desalegn H., Mulu A. 2021. Flood vulnerability assessment using GIS at Fetam watershed, upper Abbay basin, Ethiopia. Heliyon, 7(1), e05865

Elkhrachy I. 2022. Flash flood water depth estimation using SAR images, digital elevation models, and machine learning algorithms. Remote Sens. (Basel), 14, 440. https://doi.org/10.3390/RS14030440

Hagos Y., Andualem T., Yibeltal M., Mengie M. 2022. Potential floodprone area identification and mapping using GIS, MCD, Dega Damot, Ethiopia. Appl. Water Sci., 12. https://doi.org/10. 1007/ s13201- 022- 01674-8

Khosravi K., Pourghasemi H.R., Chapi K., Bahri M. 2016b. Flash flood susceptibility analysis and its mapping using different bivariate models in Iran: A comparison between Shannon's entropy, statistical index, and weighting factor models. Environ. Monit. Assess., 188, 656. https://doi.org/10.1007/s10661-016-5665-9

Lin L., Wu Z., Liang Q. 2019. Urban flood susceptibility analysis using a GIS-based multi-criteria analysis framework. Nat Hazards, 97, 455–475.

Liuzzo L., Sammartano V., Freni G. 2019. Comparison between different distributed methods for flood susceptibility mapping. Water Resour. Manag., 33, 3155–3173. https://doi.org/10.1007/s11269-019-02293-w

Master Plan for Development and Construction, Sidi Aissa. 2008.

Negese A., Worku D., Shitaye A., Getnet H. 2022. Potential flood-prone area identification and mapping using GIS-based multi-criteria decision-making and analytical hierarchy process in DegaDamot district, northwestern Ethiopia. Appl. Water Sci., 12(12), 255.

Ogato G.S., Bantider A., Abebe K., Geneletti D. 2020. Geographic information system (GIS)-based multicriteria analysis of flooding hazard and risk in Ambo Town and its watershed, West Shoa zone, Oromia Regional State, Ethiopia. J. Hydrol. Region Stud., 27, 100659

Paul G.C., Saha S., Hembram T.K. 2019. Application of the GIS-based probabilistic models for mapping the flood susceptibility in Bansloi sub-basin of Gangabhagirathi river and their comparison. Remote Sens. Earth Syst. Sci., 2, 120–146. https://doi.org/10. 1007/s41976-019-00018-6

Rahmati O., Haghizadeh A., Pourghasemi H.R., Noormohamadi F. 2016. Gully erosion susceptibility mapping: The role of GIS-based bivariate statistical models and their comparison. Nat. Hazards, 82, 1231–1258. https://doi.org/10.1007/s11069-016-2239-7

Ramesh V., Iqbal S.S. 2022. Urban flood susceptibility zonation mapping using evidential belief function, frequency ratio and fuzzy gamma operator models in GIS: a case study of Greater Mumbai, Maharashtra, India. Geocarto Intl., 37(2), 581–606.

Riazi M., Khosravi K., Shahedi K., Ahmad S., Jun C., Bateni S.M. 2023. Enhancing flood susceptibility modeling using multi-temporal SAR images, CHIRPS data, and hybrid machine learning algorithms. Sci. Total Environ. 871, 162066. https://doi.org/10. 1016/j.scitotenv.2023.162066

Saaty R.W. 1987. The analytic hierarchy process – what it is and how it is used. Mathematical Model, 9(3–5), 161–176.

Samanta S., Pal D.K., Palsamanta B. 2018b. Flood susceptibility analysis through remote sensing, GIS and frequency ratio model. Appl. Water Sci., 8, 66. https://doi.org/10. 1007/s13201-018-0710-1

Shen L., Zhang Y., Ullah S., Pepin N., Ma Q. 2021. Changes in snow depth under elevation-dependent warming over the Tibetan Plateau. Atmos. Sci. Lett., 22. https://doi.org/10.1002/asl.1041

Tehrany M.S., Pradhan B., Jebur M.N. 2015. Flood susceptibility analysis and its verification using a novel ensemble support vector machine and frequency ratio method. Stoch. Environ. Res. Risk Assess., 29, 1149–1165. https://doi.org/10.1007/s00477-015- 1021-9

Waga K., Malinen J., Tokola T. 2020. A Topographic Wetness Index for Forest Road Quality Assessment: An Application in the Lakeland Region of Finland. Forests, 11(1165), 1–13. http://dx.doi.org/10.3390/f11111165

World Health Organization report, 2023